

First-principles studies of the structural and electronic properties of poly-*para*-phenylene vinylene

This article has been downloaded from IOPscience. Please scroll down to see the full text article.

2004 J. Phys.: Condens. Matter 16 8609

(<http://iopscience.iop.org/0953-8984/16/47/013>)

View [the table of contents for this issue](#), or go to the [journal homepage](#) for more

Download details:

IP Address: 152.17.62.213

The article was downloaded on 04/04/2011 at 15:14

Please note that [terms and conditions apply](#).

First-principles studies of the structural and electronic properties of poly-*para*-phenylene vinylene

Guang Zheng¹, S J Clark, S Brand and R A Abram

Department of Physics, University of Durham, DH1 3LE, UK

E-mail: guang.zheng@durham.ac.uk

Received 13 July 2004, in final form 15 October 2004

Published 12 November 2004

Online at stacks.iop.org/JPhysCM/16/8609

doi:10.1088/0953-8984/16/47/013

Abstract

We present first-principles investigations of the structural and electronic properties of PPV in both the isolated chain and the crystalline state. The calculations are mainly based on the local density approximation within density functional theory. With this approach, we have determined the optimal structure and torsional conformation for an isolated one-dimensional polymer chain. The predicted structural and electronic properties of PPV are generally in good agreement with recent work. However, for the vinyl C=C double bond, there exists a relatively large difference ($>0.03 \text{ \AA}$) in bond length between experiment and theory, and we postulate that this arises from a bond alternation. In the crystalline state, we find that intrachain interactions are dominant, and that interchain effects play a secondary but significant role for some bands. Effective masses are calculated from the band structure, which are helpful for understanding the opto-electronic properties of the polymer, and in particular, allow us to calculate the exciton binding energy and radius.

1. Introduction

Conjugated polymers have emerged as a highly promising class of materials for electronic and optoelectronic applications, particularly for displays, light emitting diodes (LEDs), and field effect transistors (FETs) [1–3]. One polymer that has attracted considerable interest, both in terms of its basic properties and its applications, is unsubstituted poly-*para*-phenylene vinylene (PPV).

In fact, PPV has probably been the most widely studied polymer material [4–10] over the last decade. From the experimental point of view, it is easy to process and there are a number of

¹ Author to whom any correspondence should be addressed.

possible substitutions which give the opportunity to tune the optoelectronic properties. PPV is also an attractive material for the theoretical study of the properties of conjugated polymers, since it takes the form of relatively simple quasi-one-dimensional molecules arranged in a three-dimensional crystal structure. This arrangement makes it possible to study the structural and electronic properties in both the isolated chain and the crystalline states.

Although there have been rapid technological developments in the applications of PPV, many aspects of the basic physics of the polymer are not well established and its properties are not fully understood. This is in part due to the fact that realistic theoretical descriptions of the polymer involve heavy computational costs. Consequently, many calculations of the properties of PPV have been based on simple models such as that of an isolated, perfect straight chain where the solid state effects are not included. However, individual PPV chains exhibit complicated behaviour which is also significantly influenced by interchain interactions, defects, disorder, and other factors. Empirical and semi-empirical approaches can be used, but are of limited reliability, since it is often very difficult to separate the real physics from parametrization effects.

Ab initio band structure calculations have been carried out for several decades. Two main methods have been applied in these calculations; one is the Hartree–Fock (HF) approach, the other is density functional theory (DFT). The self-consistent X_α study of polyacetylene and other chain polymers has been reported by Mintmire *et al* [11]. The band structure calculations on neutral polypyrrole were performed at the HF level [12] and the results compare well with experimental spectra. Electronic and dynamic property studies have been carried out at both coupled HF [13] and post-Hartree–Fock levels for which the Møller–Plesset perturbation theory is limited to second order (MP2) [14]. The latter provides important and often dominant corrections. To find a good compromise between the computational cost and the quality of results, many-body perturbation theory (MBPT), and coupled-cluster (CC) theory have been used for extended systems [15, 16]; although non-variational, CC theory resolves the problem of size extensivity, and is often well defined, accurate and efficient. *Ab initio* electronic structure and band structure studies of polyparaphenylene (PPP) have been carried out using atom-centred basis sets [17, 18].

In this work, we study the structural and electronic properties of PPV by using first-principles calculations based on density functional theory with a plane wave representation of the electronic states and a pseudopotential description of the electron–ion interactions. In doing so, the interchain interactions can be taken into account, unlike in some previous theoretical work in which the interactions between the neighbouring chains have been neglected.

The remainder of this paper is organized as follows. Section 2 presents the structure of PPV. In section 3, the basic theory and computational technique are briefly outlined, with particular emphasis on solving for the structural and electronic properties. We present our results and discussion in section 4. A short summary concludes the paper in section 5.

2. Structures of PPV

Our study involves the following PPV-related structures as sketched in figures 1 and 2. These are the PPV repeat unit monomer (figure 1(a)), a PPV isolated chain (figure 1(b)), the styrene molecule (figure 1(c)), and the stilbene molecule (figure 1(d)).

We also study the solid state structure of PPV, where x-ray diffraction measurements [19] show that PPV has a herringbone crystal structure with a monoclinic unit cell containing two chains. The crystal structure is shown in figure 2 with $a = 8.07 \text{ \AA}$, $b = 6.05 \text{ \AA}$, and $c = 6.54 \text{ \AA}$, the monoclinic angle between b and c is 123° , the setting angle Φ is 52° , and the unit cell has $P21/a$ symmetry.

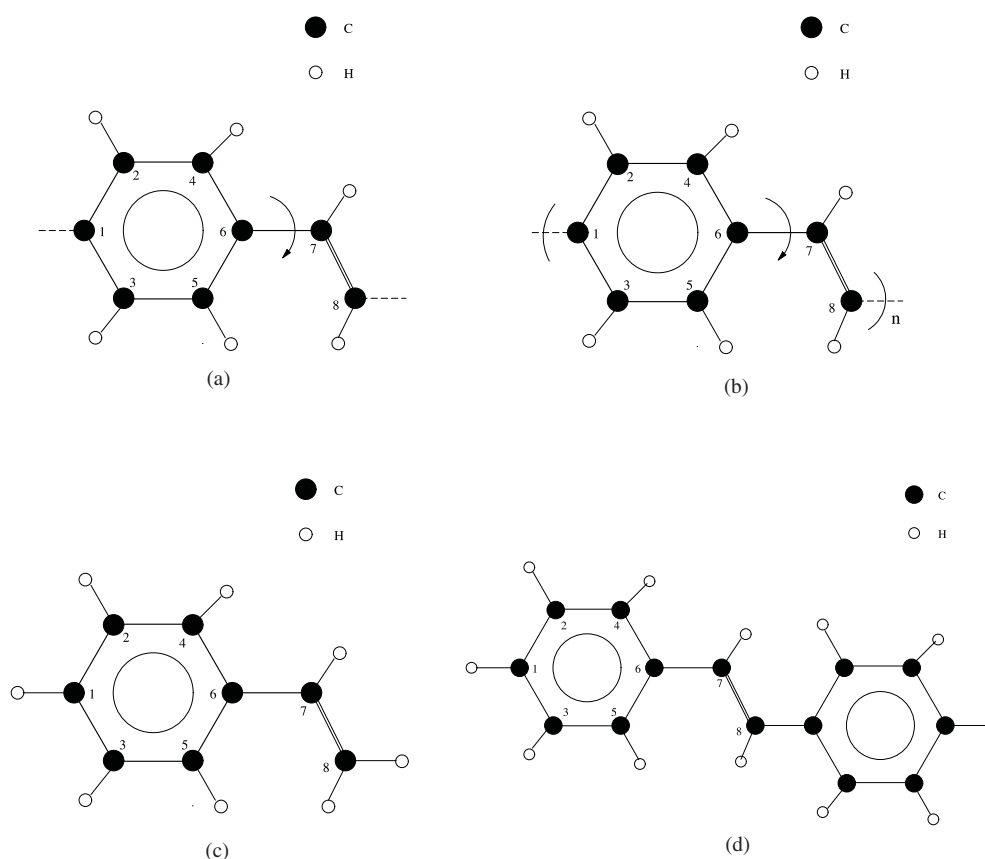


Figure 1. (a) The repeat unit (monomer) of an isolated PPV chain. The torsion angle is defined as the dihedral angle $C_4-C_6-C_7-C_8$. For convenience the labelling is consistent with that of [8]. (b) An isolated PPV chain, which is formed by the polymerization of the monomer shown. (c) A styrene molecule, which is formed when the two dangling bonds in the PPV monomer are saturated by hydrogen atoms. (d) A stilbene molecule.

3. Computational technique

Our calculations of the properties of PPV are based on density functional theory [20, 21]. In this method, the many-body exchange and correlation effects are described using the local density approximation (LDA), which has been extensively used in first-principles calculations of inorganic semiconductors. Such calculations are capable of giving accurate and reliable structural and electronic information for the ground state of the system. The calculations have been implemented using the CASTEP plane wave code [22, 23]. It is well recognized that plane wave basis sets have a number of benefits as compared to those conventionally used in quantum chemistry [23]. Further, there exists a simple parameter, the cut-off energy, for determining the degree of completeness of the basis, which gives us confidence that the wavefunction can describe the electronic properties without any particular bias [24]. The electron-ion interactions were described using the ultrasoft Vanderbilt pseudopotentials [25], which have a low cut-off energy and so reduce the number of plane waves required for the expansion of the Kohn-Sham orbitals. A cut-off energy of 380 eV was used, which ensures convergence of the total energy differences of the system to 1.0 meV/cell. The difference

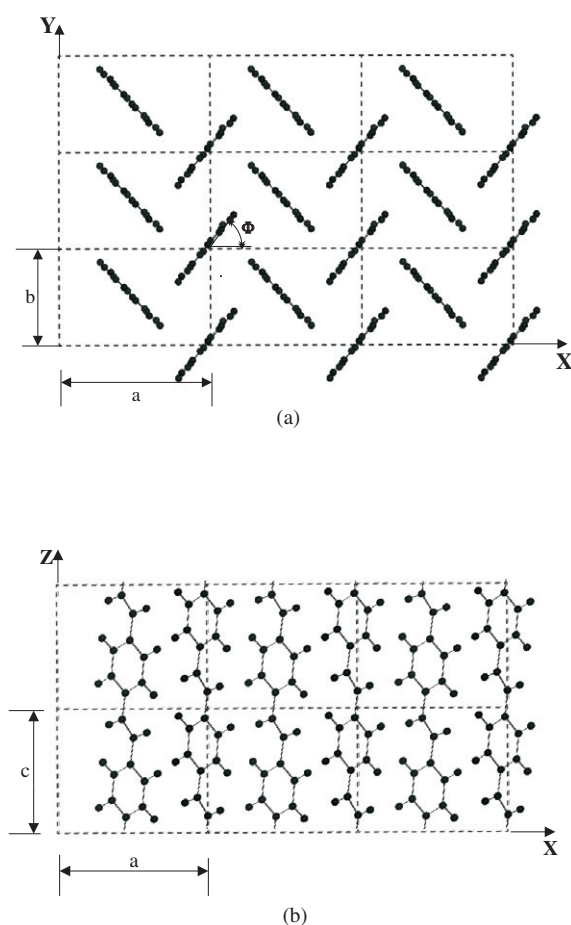


Figure 2. The herringbone crystal structure of PPV [19]. The monoclinic unit cell has $a = 8.07 \text{ \AA}$, $b = 6.05 \text{ \AA}$, $c = 6.54 \text{ \AA}$, and the angle $\Phi = 52^\circ$. (a) A top view of the polymer in the xy plane; (b) a side view of PPV in the xz plane.

between the band gap at 600 eV and that at 380 eV is less than 0.01 eV. The Monkhorst–Pack k -point sampling scheme [26] was employed to perform the k -space integrations over the first Brillouin zone to the same level of convergence. For the isolated molecule, only one k point (the Brillouin zone centre) is required; finer sampling is not necessary, since the electronic bands are effectively dispersionless for a single molecule.

Given a system (molecule or solid), its structure can be determined by a set of geometrical parameters, such as bond lengths, bond angles, and torsion angles. The optimization procedure is as follows: we first choose an initial geometry; then we calculate the Hellmann–Feynman [27] force on each atom. The atoms are moved under these forces until no force exceeds some threshold value. This allows us to find the structure that is the ‘nearest’ local minimum to the starting configuration. In our work, we use the BFGS [28] optimization method, with full relaxation taken to be when none of the ionic forces exceeds 0.05 eV \AA^{-3} , and the total energy convergence tolerance is $0.1 \times 10^{-4} \text{ eV/atom}$. The Kerker² density-mixing scheme was used to achieve self-consistency between the input and output potentials. For all these simulations, point group symmetry is not enforced since small symmetry breakings may occur.

² Kerker mixing recognizes the fact that low weighting of the small- G components of the charge density should be employed in order to prevent charge sloshing during SCF optimization.

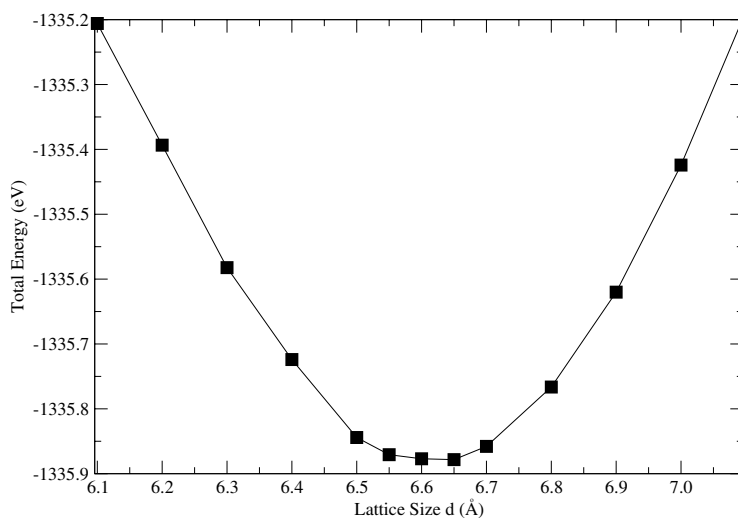


Figure 3. The ground state total energy of an isolated PPV chain as a function of the repeat size d . The optimized value of d corresponds to the minimum at 6.65 Å in the curve. The diamond squares indicate the calculated values.

4. Results and discussion

4.1. Structural properties of PPV

We first carry out calculations of the ground state structure for an isolated, infinite PPV chain, the repeat unit of which is illustrated in figure 1(a). To produce a periodic system, as required for the use of a plane wave basis set, the polymer is artificially repeated on a square lattice in the plane normal to the chain, with a sufficient distance between neighbouring chains to minimize the interchain interaction. In these calculations the dimensions of the unit cell are $10 \text{ \AA} \times 10 \text{ \AA} \times d$, where d is the repeat unit distance along the polymer chain. Then, by using the techniques described in section 3, the optimized geometry of the isolated PPV polymer chain, including the parameter d , can be obtained.

The lattice constant of the ground state is given by the location of the minimum (6.65 Å) in the total energy as a function of d , which is shown in figure 3. A selection of optimized bond lengths and bond angles, together with some experimental data and other theoretical results, are listed in table 1. For comparison, the geometrical parameters that we have calculated for a styrene molecule (see figure 1(c)) are also given in table 1. The experimental results are from x-ray diffraction studies of stilbene (figure 1(d)) molecular crystals [29]. When we compare our results for the isolated chain with those for the stilbene molecular crystals, it can be seen that our optimized geometrical parameters generally agree with the diffraction experimental data on *trans*-stilbene [29] and with some recent theoretical data [8]. However, for the vinyl $C_7=C_8$ double bond, our value for the length of 1.349 Å is 0.031 Å: greater than that observed in experiment but nevertheless closer to experiment than the value 1.361 Å found by Capaz and Caldas [8]. Interestingly, the observed $C_7=C_8$ bond length is quite close to the standard $C=C$ double-bond length of 1.33 Å [30] and our optimized value 1.329 Å in the styrene molecule. Note that the experimental value is for molecular crystals of stilbene but the calculations are for an isolated PPV chain, and it is possible that there is a bond alternation in the latter case due to the change of situation in the polymer [31].

Table 1. Selected geometrical parameters of an isolated PPV chain. Bond lengths and angles are in Å and degrees, respectively. Carbon atom labels are the same as in figure 1. The experimental data are x-ray diffraction values for *trans*-stilbene molecular crystals [29]. Reference [8] is concerned with the optimized geometry in a first-principles calculation for an isolated PPV chain. For comparison, the parameters for a styrene molecule are also given.

Parameters	Isolated chain ^a	Isolated chain ^c	Experiment ^d	Styrene ^b
C ₂ -C ₄	1.375	1.383	1.387	1.381
C ₁ -C ₂	1.401	1.411	1.397	1.384
C ₁ -C ₃	1.403	1.414	1.394	1.395
C ₆ -C ₇	1.451	1.443	1.469	1.449
C ₇ -C ₈	1.349	1.361	1.318	1.329
C ₂ -H	1.096	1.103	0.93	1.095
C ₃ -H	1.096	1.104	1.02	1.096
C ₇ -H	1.101	1.108	1.00	1.098
C ₂ -C ₁ -C ₃	116.7	117.3	117.8	119.6
C ₁ -C ₂ -C ₄	120.9	121.1	121.4	119.7
C ₁ -C ₃ -C ₅	122.4	121.6	120.6	120.7
C ₆ -C ₇ -C ₈	127.0	126.3	126.7	128.0
C ₁ -C ₂ -H	119.9	119.4	117.2	120.2
C ₁ -C ₃ -H	117.9	118.7	119.0	119.6
C ₆ -C ₇ -H	114.6	115.0	116.1	113.5

^a This work, for the isolated PPV chain.

^b This work; optimized parameters for a styrene molecule.

^c Reference [8]; DFT optimized geometry for an isolated PPV chain.

^d X-ray scattering for *trans*-stilbene molecular crystals [29].

Total energy calculations for an isolated PPV chain were performed in which the torsion angle C₄-C₆-C₇-C₈ is constrained to particular values in order to obtain the energies of different torsional conformations of PPV. Note that the 0° and 180° rotations correspond to the *cis* and *trans* conformations, respectively. The results for the total energy as a function of torsion angle in figure 4 suggest that the ground state has a planar configuration. The predicted planarity of PPV is not quite in agreement with the experimental diffraction data [19, 32], which suggests a torsion angle of approximately 5° that increases somewhat with temperature. In the PPV chain, there are two competing tendencies: on the one hand, extended π conjugation is best achieved if the polymer chain adopts a planar conformation, but there also exists a steric repulsion between the adjacent phenylene ring and the vinylene hydrogen atoms, which favours a non-planar construction. The balance between these two effects results in a non-zero torsion angle in the PPV chain. However, the observed deviation from planarity is for a crystal and not the isolated chain. It is difficult to confirm the 5° torsion angle theoretically, since the energy difference between the planar and non-planar conformations is very small. For example, for an isolated infinite PPV chain, we have calculated the energy difference between the planar and 5° conformations to be less than 1 meV/cell.

4.2. Electronic properties of PPV

4.2.1. Isolated chain. There are eight carbon atoms in a PPV chain repeat unit but only one electron per atom takes part in the conjugated π bonding. Since each band can hold exactly two electrons, the four π valence bands with the lowest energy are filled and the four π^* conduction bands above them are empty. Three of the four π bands belong to the benzene ring, and the corresponding wavefunctions are delocalized along the chain. The other π band derives mainly from the vinylene states, and the corresponding wavefunctions are localized on the vinyl C=C double bond.

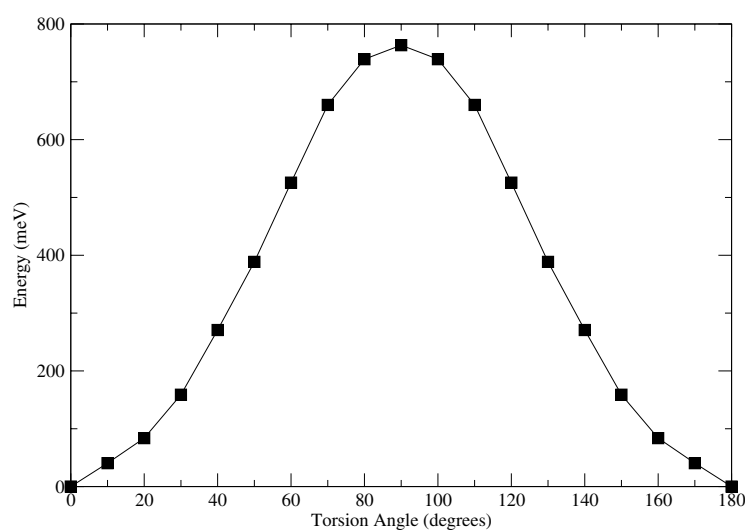


Figure 4. The torsional potential energy (in meV) for an isolated PPV chain as a function of the torsion angle, which suggests a planar ground state. The squares are the calculated data.

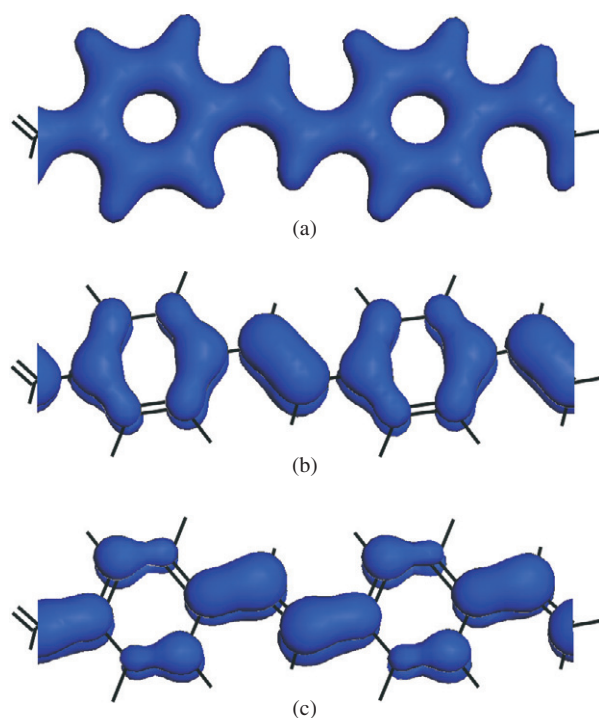


Figure 5. Charge densities of an isolated PPV polymer chain (isosurfaces of densities are shown at $0.1e \text{ \AA}^{-3}$). (a) The isosurface of total charge density; (b) the isosurface of the HOMO charge density; (c) the isosurface of the LUMO charge density.

(This figure is in colour only in the electronic version)

The total electronic charge density isosurface, set at $0.1e \text{ \AA}^{-3}$, for an isolated PPV chain is shown in figure 5(a). It can be seen that the total charge density in the plane of the backbone is equally distributed in the benzene ring and the vinyl linkage, as expected. The charge densities for the highest occupied molecular orbital (HOMO) and the lowest unoccupied molecular orbital (LUMO) are shown in figure 5(b) and figure 5(c), respectively, and it is found that for both the HOMO and the LUMO there is a much smaller charge density on the hydrogen atoms. This result is in good agreement with the work of da Costa *et al* [33].

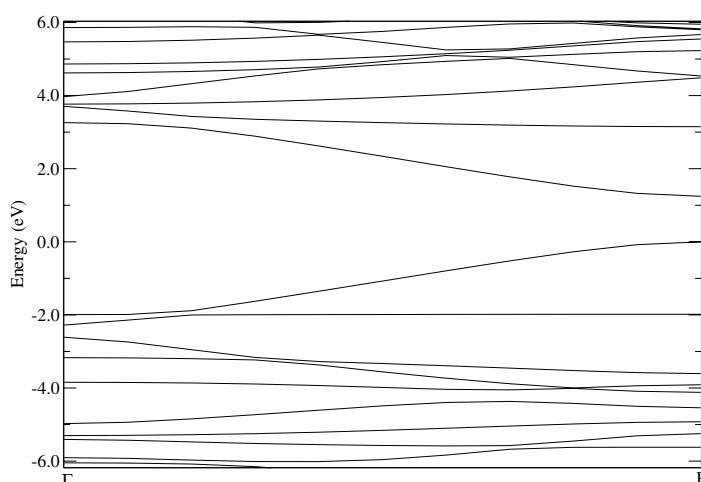


Figure 6. The DFT/LDA band structure for an isolated PPV chain. The energies are measured relative to the top HOMO at the P point in the Brillouin zone.

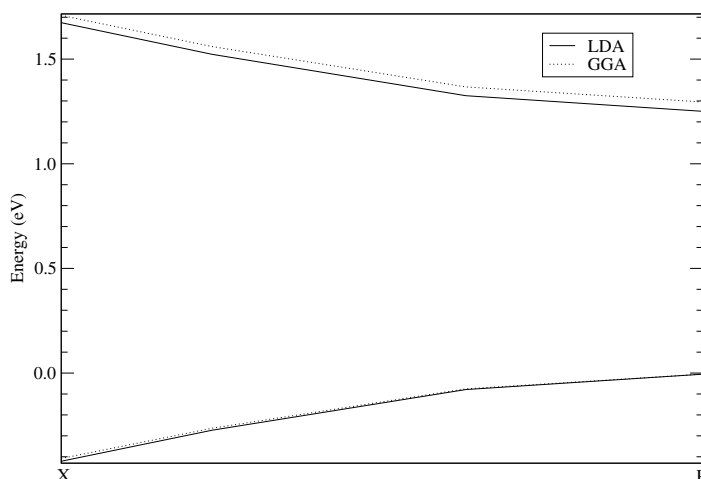


Figure 7. The band structure showing the HOMO and LUMO of an isolated PPV chain (LDA versus GGA). This figure is scaled to highlight the difference between the LDA and GGA. The main features of the GGA band structure are similar to those of the LDA in figure 6. The energies are measured relative to the top HOMO at P.

The electronic band structure for the isolated chain of PPV is shown in figure 6. This single-particle band structure exhibits an energy band gap of 1.3 eV between the HOMO and the LUMO. This is considerably less than the optical gap of 2.4 eV that has been measured experimentally by Voss *et al* [34]. The general tendency of approximate schemes, such as LDA and GGA, in the DFT approach is to underestimate band gaps, often by 50% or more. Figure 7 compares the results of LDA and GGA calculations, in which the revised Perdew–Burke–Ernzerhof (RPBE) functional [35] was used to account for the exchange–correlation effects. It is apparent that LDA and GGA exhibit quite similar features; the largest dispersion of about 2.0 eV occurs in the chain direction Γ P, and GGA slightly improves the band gap at P. However, the predicted value is much too small and differs by less than 0.1 eV compared to the LDA. The underestimation of the electronic band gap is partly due to the local or semi-local

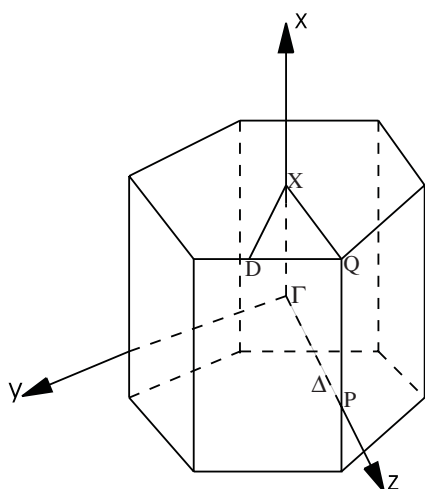


Figure 8. The Brillouin zone of the PPV polymer crystal. The symmetry labels are consistent with those of [33]. Δ is in the chain direction from Γ to P and lies 0.7 of the way along Γ P.

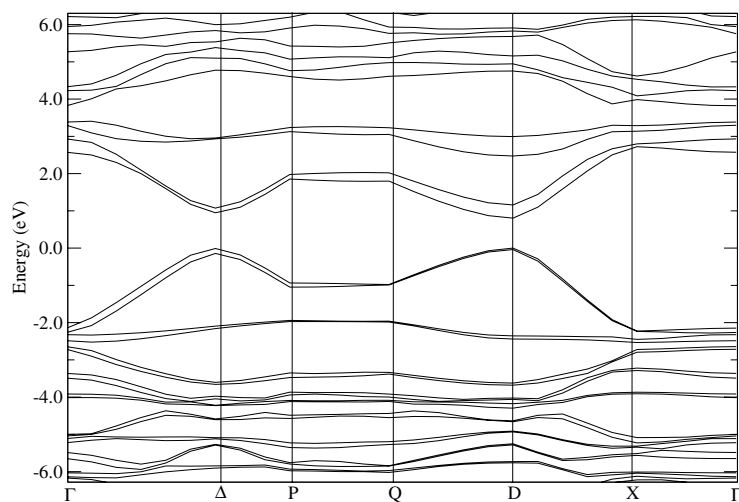


Figure 9. The band structure for the PPV polymer crystal. Energies are in electronvolts relative to the top HOMO. The symmetry labels are defined in figure 8.

nature of the LDA (and GGA) functionals and a non-local density functional treatment of the isolated polymer chain can be expected to give rise to greatly improved results [36].

4.2.2. Crystalline state. The Brillouin zone of the crystalline polymer is shown in figure 8 and the calculated band structure is presented in figure 9. Compared with the band structure of the isolated chain, the main difference is that the bands occur in pairs. This is due to the two chains per unit cell in the herringbone crystal structure of undoped PPV, which would result in doubly degenerate bands if it were not for the small splittings due to interchain interactions. As a matter of fact, similar features have been found previously in crystalline *trans*-(CH)_n [37]. The C–H interaction between neighbouring chains [33, 38] is mainly responsible for the splitting of bands shown in figure 9. The effect of interchain interactions can also be seen in the density of states (DOS) for the crystalline state when compared with that of an isolated chain. The total DOS of an isolated PPV chain is plotted in figure 10, and that for the PPV crystalline state in figure 11. It is found that the general features of the two densities of states are quite similar for the valence band, but there are more small peaks (due to the two chains per unit

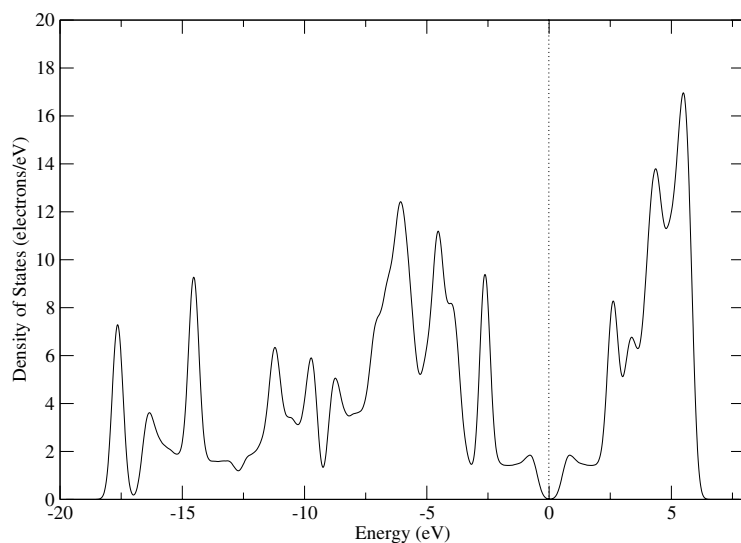


Figure 10. The total density of states for an isolated PPV polymer chain. The vertical dotted line indicates the position of the Fermi level. The energies have been Gaussian broadened.

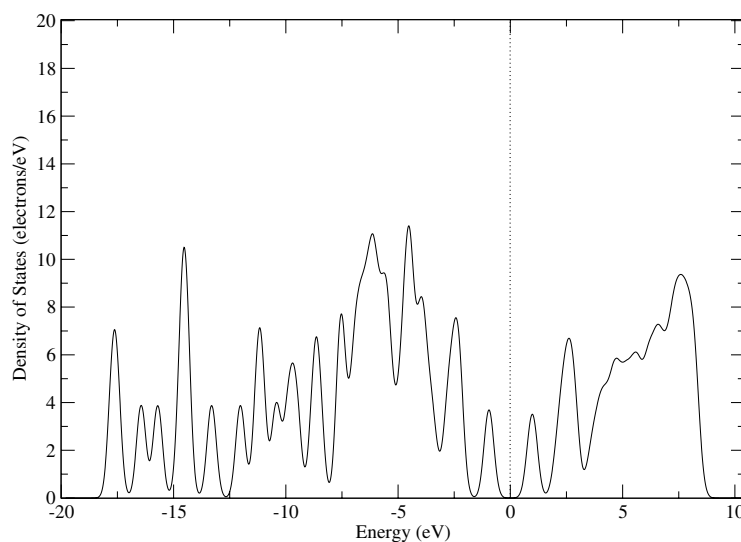


Figure 11. The total density of states for PPV in the crystalline state. The vertical dotted line indicates the position of the Fermi level. Gaussian broadening has been used on the binned energies.

cell) for the crystalline DOS. However, in the upper valence and conduction bands, especially in the vicinity of 5 eV, the DOS for the crystal structure is much smaller and quite a lot broader, indicating that the interchain interactions have a larger influence on the crystalline DOS in this region. It is evident that the electronic properties of conjugated polymers depend sensitively on the physical conformation of the polymer chains and the way the chains pack together in bulk films as discussed by Schwartz [39].

The small splittings and band pairs were not observed in the calculations of van der Horst *et al* [7], in which a dielectric medium was used to model the interchain interactions but the effect of the crystalline packing was not taken into account. The largest band dispersion occurs along the chain direction ΓP , with a value of about 2.1 eV, which is similar to that for the isolated chain. The bands are quite flat in the directions perpendicular to ΓP (such as PQ and ΓX), implying that the interchain interactions are small compared with the intrachain interactions.

Table 2. Effective mass tensor components (in units of the free electron mass) obtained from the calculated PPV crystal band structure.

Points	Bands	x	y	z
Δ	HOMO	10.95	-1.94	0.09
	LUMO	-3.80	-11.18	0.13
Γ	HOMO	4.18	-2.09	-0.18
	LUMO	2.52	1.03	-0.33

However, it can be found that different bands experience quite different interchain coupling effects. For example, the lowest conduction band (LUMO) has a bigger splitting and is more dispersive along QX than the highest valence band (HOMO), indicating that the interchain interaction has more influence on the LUMO. The minimum band gap occurs at D (with a slightly larger gap at Δ) and is about 0.3 eV smaller than the gap of the isolated chain. Also at Δ and D the HOMO and LUMO bands are well separated from the other bands.

It is useful to compute the effective mass tensor for relevant bands from the dispersion curves of the band structure. This is one of the most important quantities used in the analysis of experimental results and in theoretical modelling, as, for example, when considering excitonic effects. The effective mass tensor is defined as $1/m(\mathbf{k})_{i,j} = \pm \partial^2 E(\mathbf{k})/(\hbar^2 \partial k_i \partial k_j)$, where + applies for electrons and the minus sign for holes. We have calculated the tensor components in the three principal directions **x**, **y**, and **z** (see figure 8) for the HOMO and LUMO bands at Γ and Δ and the results are summarized in table 2. It can be seen that the effective mass components in the chain direction are quite similar at Δ and Γ , and at Δ the HOMO and LUMO bands are more dispersive in the **x** directions. The magnitude of the effective mass parallel to the chain is smaller than those in the other two directions but only by one or two orders of magnitude. This indicates that the interchain interactions also contribute significantly to the crystalline packing effects [10]. Using the effective mass $0.09 m_e$ in table 2 and the definition for the binding energy of a hydrogenic-like state in a one-dimensional system [40], we can estimate the exciton binding energy associated with the lowest electronic LUMO–HOMO transition. The resulting binding energy is about 0.2 eV and the exciton radius is approximately 20 Å. Such values are reasonable when compared with the exciton binding energy, in the range of 0.2–0.6 eV, measured by scanning tunnelling spectroscopy [41].

5. Summary and conclusions

We have investigated the structural and electronic properties of the semiconducting conjugated polymer PPV in the isolated and crystalline states. Our predictions of the structural properties are generally in good agreement with the experimental data and other recent theoretical work. However, for the double-bonded $C_7=C_8$ vinyl bond, there is a relatively large difference between the theoretical result and the experimental value. As a result, we postulate that this bond may undergo a bond alternation in the polymer state. The calculated electronic properties of an isolated chain agree well with the other available theoretical data. The band gaps of PPV are in good agreement with those from previous works. The investigation of the band structure of the crystalline material has allowed us to study certain solid state effects, and we have demonstrated the existence of small splittings in the bands arising from interchain interactions. Although intrachain interactions are dominant, the interchain effects play a significant role for some bands. Effective mass parameters have been obtained for the HOMO and LUMO bands, which may be used in models of electronic and optical phenomena in PPV.

Acknowledgments

We acknowledge the financial support of EPSRC grant GR/R56716/01 and are grateful for the allocation of computing time on the HPCx computer of Daresbury Laboratories through the UKCP consortium. G Zheng is grateful for helpful discussions with C H Patterson.

References

- [1] Burroughes J H, Bradley D D C, Brown A R, Marks R N, Mackay K, Friend R H, Burns P L and Holmes A B 1990 *Nature* **347** 539
- [2] Gelinck G H, Geuns T C T and de Leeuw D M 2000 *Appl. Phys. Lett.* **77** 1487
- [3] Drury C J, Mutsaers C M J, Hart C M, Matters M and de Leeuw D M 1998 *Appl. Phys. Lett.* **73** 108
- [4] Hide F, Diaz-Garcia M A, Schwartz B J, Andersson M R, Pei Q and Heeger A J 1996 *Science* **273** 1833
- [5] Brédas J L, Beljonne D, Cornil J, Calbert J P, Shuai Z and Silbey R 2002 *Synth. Met.* **125** 107
- [6] Rohlfling M and Louie S G 1999 *Phys. Rev. Lett.* **82** 1959
- [7] van der Horst J W, Robert P A, Michaels M A J, Brocks G and Kelly P J 1999 *Phys. Rev. Lett.* **83** 4413
- [8] Capaz R B and Caldas M J 2003 *Phys. Rev. B* **67** 205205
- [9] Ruini A, Caldas M J, Bussi G and Molinari E 2002 *Phys. Rev. Lett.* **88** 206403
- [10] Ferretti A, Ruini A, Molinari E and Caldas M J 2003 *Phys. Rev. Lett.* **90** 086401
- [11] Mintmire J W and White C T 1983 *Phys. Rev. Lett.* **50** 101
- [12] André J M, Vercauteren D P, Street G B and Brédas J L 1984 *J. Chem. Phys.* **80** 5643
- [13] Kirtman B, Gu F L and Bishop D M 2000 *J. Chem. Phys.* **113** 1294
- [14] Poulsen T D, Mikkelsen K V, Fripiat J G, Jacquemin D and Champagne B 2001 *J. Chem. Phys.* **114** 5917
- [15] Sun J Q and Bartlett R J 1996 *Phys. Rev. Lett.* **77** 3669
- [16] Hirata S, Podeszwa R, Tobita M and Bartlett R J 2004 *J. Chem. Phys.* **120** 2581
- [17] Miao M S, Van Camp P E, Van Doren V E, Ladik J J and Mintmire J W 1998 *J. Chem. Phys.* **109** 9623
- [18] Champagne B, Mosley D H, Fripiat J G and André J M 1996 *Phys. Rev. B* **54** 2381
- [19] Chen D, Winokur M J, Masse M A and Karasz F E 1990 *Phys. Rev. B* **41** 6759
- [20] Hohenberg P and Kohn W 1964 *Phys. Rev.* **136** B864
- [21] Kohn W and Sham L J 1965 *Phys. Rev.* **140** A1133
- [22] Payne M C, Teter M P, Allan D C, Arias T A and Joannopoulos J D 1992 *Rev. Mod. Phys.* **64** 1045
- [23] Segall M D, Lindan P J D, Probert M J, Pickard C J, Hasnip P J, Clark S J and Payne M C 2002 *J. Phys.: Condens. Matter* **14** 2717
- [24] Clark S J, Ackland C J and Grain J 1998 *Europhys. Lett.* **44** 578
- [25] Vanderbilt D 1990 *Phys. Rev. B* **41** 7892
- [26] Monkhorst H J and Pack J D 1976 *Phys. Rev. B* **13** 5188
- [27] Hellmann J 1937 *Einführung in Die Quantenchemie* (Leipzig: Deuticke)
- [28] Feynman R P 1939 *Phys. Rev.* **56** 340
- [29] Broyden C G 1970 *J. Inst. Math. Appl.* **6** 76
- [30] Fletcher R 1970 *Comput. J.* **13** 317
- [31] Goldfarb D 1970 *Math. Comput.* **24** 23
- [32] Shanno D F 1970 *Math. Comput.* **24** 647
- [33] Finder C J, Newton M G and Allinger N L 1974 *Acta Crystallogr. B* **30** 411
- [34] MacGillavry C H and Rieck G D (ed) 1962 *International Tables for X-ray Crystallography* vol 3 (Birmingham: Kynock)
- [35] Hjort M and Stafström S 2000 *Phys. Rev. B* **62** 5245
- [36] Chen D, Winokur M J, Masse M A and Karasz F E 1992 *Polymer* **33** 3116
- [37] Gomes da Costa P, Dandrea R G and Conwell E M 1993 *Phys. Rev. B* **47** 1800
- [38] Voss K F, Foster C M, Smilowitz L, Mihailovic D, Askari S, Srdanov G, Ni Z, Shi S, Heeger A J and Wudl F 1991 *Phys. Rev. B* **43** 5109
- [39] Hammer B, Hansen L B and Nørskov J K 1999 *Phys. Rev. B* **59** 7413
- [40] Zheng G, Clark S J, Brand S and Abram R A 2004 at press
- [41] Vogel P and Campbell D K 1990 *Phys. Rev. B* **41** 12797
- [42] Ambrosch-Draxl C, Majewski J A, Vogel P and Leising G 1995 *Phys. Rev. B* **51** 9668
- [43] Schwartz B J 2003 *Annu. Rev. Phys. Chem.* **54** 141
- [44] Heeger A J 2001 *Rev. Mod. Phys.* **73** 681
- [45] Alvarado S F, Seidler P F, Lidzey D G and Bradley D D C 1998 *Phys. Rev. Lett.* **81** 1082
- [46] Rossi L, Alvarado S F, Reiss W, Schrader S, Lidzey D G and Bradley D D C 2000 *Synth. Met.* **111/112** 527